A NEUROALGORITHMIC INVESTIGATION OF THE OUTER RETINA

Tomás Maul, Andrzej Bargiela and Lee Jung Ren
School of Computer Science
University of Nottingham Malaysia Campus
Malaysia
Email: Tomas.Maul@nottingham.edu.my

KEYWORDS

Retinal Models; Multi-Resolution Recurrent Neural Networks; Optimization; Image Processing.

ABSTRACT

In this paper a new model of the Outer Plexiform Layer (OPL) of the human retina is presented. The model, which is a multi-resolution Linear Recurrent Neural Network (LRNN) defined by 31 parameters, was subjected to several optimization experiments targeting different low-level visual functions involving the control of noise, brightness, contrast, saturation and color. Our results indicate that the model can indeed implement the above image processing functions and that the solutions can be modulated in different ways. The model provides a good starting point for extensions targeting real world applications and for the generation of testable biological hypotheses.

INTRODUCTION

The retina is arguably one of the most extensively studied neural structures in the primate nervous system. In spite of this, many open problems regarding both the structure and function of the retina remain to be addressed. For example, the precise number of different horizontal cell (HC) types in the primate retina is still a matter of debate (Kolb et al., 1994). Furthermore, the precise connectivity patterns between different photoreceptor and HC types is still unclear. Added to this, the retina's representational, coding and computational functions have yet to be completely revealed (Field and Chichilnisky, 2007). In a similar vein, but now in the context of computer applications, the field of Image Processing is one where the maturity of the field does not entail any shortage of open problems. It is hard to identify an image processing function (e.g. denoising or colour correction) that can't benefit from further improvement, be it in terms of accuracy, speed or adaptability. Refer to (Egmont-Petersen et al., 2002) for a useful review of Artificial Neural Network (ANN) solutions to Image Processing problems.

The primate retina consists of five main cell types, i.e.: photoreceptor (PR), horizontal, bipolar, amacrine and retinal ganglion cells. Each one of these types consists of several sub-types, such that the retina can be seen to consist of 55 distinct neurons subtypes in total (Masland, 2001). Two main layers of neuronal interconnections, the Outer Plexiform Layer (OPL) and the Inner Plexiform Layer (IPL) carry out the bulk of retinal processing. The current paper focuses on the OPL seeing that, in spite of its greater simplicity and thus modeling viability, it still presents us with several open problems. Furthermore, accurate modeling of the OPL output (and thus IPL input), can be seen as a pre-requisite for modeling the latter.

Efforts related to the modeling or emulation of biological retinas is not new and can be classified into the following three categories, ordered from the most biologically concerned to the most engineering based: 1) computational neuroscience modeling (Wohrer et al., 2006), 2) software based image processing (Ebner, 2006) and 3) hardware based image processing (Zaghloul and Boahen, 2006). Although these efforts have contributed to addressing some biological questions and advancing image processing to some extent, as we have mentioned challenges remain. To the best of our knowledge, our model of the OPL is the first one to include detailed chromaticity-specific connection patterns between PRs and HCs, with the possibility of distinct patterns for different HC types.

Our approach lies at the intersection of Computational Neuroscience and Natural Computation. For the sake of simplicity, this intersection will be hereafter referred to as Neuroalgorithmics. This relatively old but newly named field is concerned both with the modeling of biological neural systems and the extraction of biologically inspired algorithms. It is hoped that the explicit pursuit of this dual concern will provide us with a new framework and methodologies for solving some of the remaining open problems in vision science.

Because retinal models are generally considered large scale models it was not practical to use multi-compartmental modeling techniques. Furthermore, because the OPL is generally interpreted as a linear filter and contains feedforward, lateral and recurrent connections, we decided to simplify its representation via a Linear Recurrent Neural Network (LRNN) (Haykin, 2008). The LRNN model is represented by a set of 31 parameters. As mentioned in (Schutter, 2009) some modeling studies are motivated by unknown input/output relationships, while others are motivated by unknown structural elements (e.g. connectivity). In the OPL case, there

Proceedings 24th European Conference on Modelling and Simulation ©ECMS Andrzej Bargiela, Sayed Azam Ali
David Crowley, Eugène J.H. Kerckhoffs (Editors)
ISBN: 978-0-9564944-0-5 / ISBN: 978-0-9564944-1-2 (CD)

is partial and incomplete understanding of both aspects. The parameterization allows for flexible generation of different OPL network configurations which potentially can help us reveal structural aspects. The optimization of the network parameters viz a viz different low-level visual functions, helps address questions related to input/output relationships.

The primary objective of the work reported in this paper is to extract a useful neural solution from nature, that is accurate, compact, efficient, parallelizable, flexible (i.e. implements different visual functions), adaptable (i.e. allows for simple modulation), extensible and theoretically tractable. The secondary objective of the work is to generate reasonable hypotheses or useful questions pertaining to the biological retina.

The following section will discuss the methods adopted in more detail (e.g. the model and optimization framework). Experimental results will be presented in the subsequent section demonstrating several properties of the LRNN. The final section will analyze the results, evaluate the LRNN with reference to the work's objectives, and offer several conclusions and directions for future work.

METHODS

The Model

The model reported in this paper is essentially an OPL-inspired LRNN. The main OPL elements incorporated in the model include: different types of cone photoreceptors (PR), inter-cone gap junctions (GJ), different types of horizontal cell, inter-HC gap junctions, feedforward connections from PRs to HCs, feedback connections from HCs to PRs, local HC receptive fields and variable proportions of connections between different PR types and HCs. Omitted OPL elements include: rods, nonlinearities of cell potentials and complex temporal dynamics. Other simplifications include the representation of light as image pixels and the assignment of three cones per image pixel. The abstraction choices that were made reflect our intention to generate plausible hypotheses pertaining to the functional consequences of GJs and cone/HC connectivity patterns and to efficiently test the functional diversity of the network.

The structure and function of the LRNN is represented by a set of 31 parameters. Table 1 depicts these parameters and provides brief descriptions for each one. The value of each parameter belongs to the range $[0, 1]$. For attributes whose values belong to the set of natural numbers (e.g. maximum iterations), another parameter is used to represent the actual maximum value of that attribute. In this case, the value in Table 1 (e.g. parameter 31) represents a proportion and the actual value of the attribute is computed via the function $r(p_i \times max_i)$, where r is the rounding function, p_i represents the value of parameter i and max_i represents the actual maximum value of attribute i. Maximum values are defined for the following three attributes: maximum number of iterations, HC input radius and HC output radius. The notation HC_n denotes the horizontal cell with index n. The multi-resolution property of the LRNN is a result of the fact different HC types may receive/send information from/to the PR layer at different resolutions.

Table 1: LRNN parameter descriptions.

P1	Weight of the influence of light on cones
P2	Weight of a cone's influence on itself
P3	Cone GJ weight: intra-positional and inter-chromatic
P4	Cone GJ weight: inter-positional and intra-chromatic
P5	Cone GJ weight: inter-positional and inter-chromatic
P6	Radius of input from the PR layer onto HC1 cells
P7	Radius of output from HC1 cells to the PR layer
P8	Proportion of synapses from red cones onto HC1 cells
P9	Proportion of synapses from green cones onto HC1 cells
P10	Proportion of synapses from blue cones onto HC1 cells
P11	Relative connection weights from PRs onto HC1 cells
P12	Relative connection weights from HC1 cells onto PRs
P13	Radius of input from the PR layer onto HC2 cells
P14	Radius of output from HC2 cells to the PR layer
P15	Proportion of synapses from red cones onto HC2 cells
P16	Proportion of synapses from green cones onto HC2 cells
P17	Proportion of synapses from blue cones onto HC2 cells
P18	Relative connection weights from PRs onto HC2 cells
P19	Relative connection weights from HC2 cells onto PRs
P20	Radius of input from the PR layer onto HC3 cells
P21	Radius of output from HC3 cells to the PR layer
P22	Proportion of synapses from red cones onto HC3 cells
P23	Proportion of synapses from green cones onto HC3 cells
P24	Proportion of synapses from blue cones onto HC3 cells
P25	Relative connection weights from PRs onto HC3 cells
P26	Relative connection weights from HC3 cells onto PRs
P27	Weight of an HC's influence on itself
P28	HC GJ weight: same position, different HC type
P29	HC GJ weight: different position, same HC type
P30	HC GJ weight: different position, different HC type
P31	Number of iterations

Equation 1 encapsulates the update rule for the PR layer. As the equation shows, the main inputs to any PR cell originate from light, the cell itself and nearby PR and HC cells:

$$b_{ip}^{t+1} = w_1 a_{ip}^t + w_2 b_{ip}^t + w_3 \sum_{j \neq i} b_{jp}^t + w_4 \sum_{p' \in n(p)} b_{ip'}^t + \\ + w_5 \sum_{\substack{j \neq i \\ p' \in n(p)}} b_{jp'}^t - \sum_{h \in H} w_h \left(\sum_{(hp') \in v(ip)} c_{hp'}^t \right) \quad (1)$$

where a, b and c represent light intensity, PR cell activity, and HC cell activity respectively, t denotes time, i and

j index chromaticity, p and p' index position and h represents HC type. The set of neighbours $n(p)$ is defined in Equation 2 while the set of connections $v(ip)$ is defined in Equation 3. Influence weights are denoted by w_i where the subscript refers to the corresponding parameter i in Table 1. The weight w_h represents the influence of HC cells of type h on PR cells. Although weights are based on their corresponding parameters, actual weights are normalized by the total sum of weights used in a particular cell update.

$$n(p) = \{p' \mid p' \neq p \wedge d(p'_x, p_x) \leq r \wedge d(p'_y, p_y) \leq r\} \tag{2}$$

where $d(p'_x, p_x)$ represents the distance between positions p and p' along the x-axis and r represents the *radius* of GJ influence.

$$v(ip) = \{(h, p') \mid con(PR_{pi}, HC_{hp'}) \equiv 1\} \tag{3}$$

where $con(c_1, c_2) \equiv 1$ denotes that a feedforward connection exists from cell c_1 to cell c_2.

Equation 4 encapsulates the update rule for the HC layer:

$$c^{t+1}_{hp} = w_{h'} \left(\sum_{(ip') \in v(hp)} b^t_{ip'} \right) + w_{27} c^t_{hp} + w_{28} \sum_{k \neq h} c^t_{kp} + \\ + w_{29} \sum_{p' \in n(p)} c^t_{hp'} + w_{30} \sum_{\substack{k \neq h \\ p' \in n(p)}} c^t_{kp'} \tag{4}$$

where b, c, t, i, p, p', w_i and $n(p)$ are defined as before, k represents HC type, $v(hp)$ is defined in Equation 5 and $w_{h'}$ represents the weighted influence of PR cells on HC cells of type h.

$$v(hp) = \{(i, p') \mid con(PR_{ip'}, HC_{hp}) \equiv 1\} \tag{5}$$

The connectivity between PRs and different HC types is characterized by distinct weights, input/output radii and proportions of red, green or blue cones (see Table 1: P6 to P26). The model makes use of connectivity templates (one for each HC type), which are repeatedly used over the whole space of cells.

Initialization of the network is performed through a simple sequential activation process, whereby first the inputted image (i.e. "light") is copied to the PR layer and then the activities of the cells in the HC layer are computed by taking into account PR activities and PR-to-HC connections only (i.e. HC GJs are ignored at this stage).

Optimization

The simplified model of the OPL as characterized by the 31 LRNN parameters, was subjected to several optimization experiments. In each experiment the model (or parameter set) was optimized relative to a different low-level visual function, i.e.: ↓ noise, ↑↓ brightness, ↑↓ contrast, ↑↓ saturation and ↑↓ redness, where ↑ denotes *increase* and ↓ denotes *decrease*. In general, if a visual function involves increasing measure m (e.g. contrast) then optimization with regards to that function is implemented via a cost function that takes as input a source and a target image, where the latter corresponds to the former with increased m, and computes the distance between the output of the LRNN (as defined by the parameter set) and the target image. All images used in the optimization were of resolution 100×100. After optimization, the LRNN targeting a new visual function, is almost invariably a new set of parameters and thus a new neural network structure/function.

Optimization was performed using a Global Stochastic Optimization (GSO) algorithm, combining elements of Differential Evolution Storn and Price (1997) and Genetic Algorithms Goldberg (1989). At each iteration, the population of solutions is first expanded through mutation and cross-over, then ranked, after which new solutions are generated based on the differences between strong and weak solutions. Solutions are then ranked and trimmed keeping both quality and diversity in mind. Optimization continues until either a certain maximum number of iterations or a particular cost has been reached. For lack of space we will not delve into further details of the GSO. Note that although our optimization approach is a hybrid, we have no reason to believe that other GSO approaches should be less successful in finding useful parameter configurations.

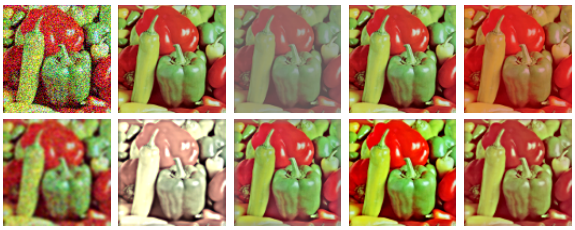

Figure 1: Processing examples.

RESULTS

Figure 1 contains examples of the processing capabilities of the OPL model. The top row depicts input images whereas the bottom row depicts corresponding output (processed) images (extracted from the PR layer). From left to right images were processed with network configurations that were optimized for the following functions: ↓ noise, ↑ brightness, ↑ contrast, ↑ saturation and ↓ redness.

Although the optimization cost functions were designed around single images, Table 2 demonstrates that the resulting network configurations are general enough to suitably handle new images. For each visual function (e.g. ↓ noise), the corresponding solution was tested on

Table 2: Some generalization results.

Function	% Correct	Mean	Max.
↓ Noise	100	−3.04	−4.18
↑ Brightness	60	−0.02	0.04
↓ Brightness	70	−0.05	−0.15
↑ Contrast	100	0.75	0.94
↓ Contrast	100	−0.12	−0.35
↑ Saturation	100	0.12	0.16
↓ Saturation	100	−0.1	−0.13
↑ Redness	70	0.0003	0.0011
↓ Redness	60	−0.0003	−0.0010

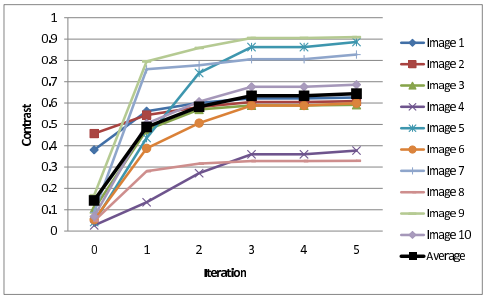

Figure 2: Multiple iterations of contrast enhancement.

ten different images. The second column from the left depicts the percentage of images that were correctly processed for each function. The definition of "correct processing" is relative to a non-reference measure for the visual function under consideration. For example, in the ↓ noise case, if the *noise* of the output image is lower than that of the input, then the processing is considered to be correct. The third column from the left depicts the mean measure differences ($output - input$) for each corresponding function, whereas the last column depicts the most significant difference.

Table 3 depicts parameter configurations optimized for five different functions. The functions from left (↓N) to right (↓S) are: decrease noise, increase contrast, decrease contrast, increase saturation and decrease saturation.

The fact that the LRNN is stable can be observed in Figures 2 and 3. These graphs also demonstrate how different quantities (e.g. contrast) can be fine-tuned by applying multiple iterations. Iteration 0 depicts the contrast (or saturation) measures of the input images. Notice how in the saturation case, the processing measure at the last iteration is more predictable from iteration 0 than in the contrast case.

Apart from the application of multiple iterations (e.g. Figure 2), fine-graded control over visual functions can also be obtained from parameter modulation. Figures 4 and 5 show several relevant parameters, whose modulation leads to predictable changes in terms of contrast. The first figure depicts parameters that are directly pro-

Table 3: Parameters optimized for different functions.

Param.	↓N	↑C	↓C	↑S	↓S
P1	0.12	0.78	0.00	0.87	0.95
P2	0.84	0.53	0.00	0.32	1.00
P3	0.11	0.00	0.00	0.00	0.34
P4	0.44	0.03	0.00	0.05	0.00
P5	0.00	0.00	0.57	0.00	0.00
P6	0.17	0.57	0.00	1.00	0.27
P7	0.66	0.94	0.28	0.62	0.00
P8	0.28	0.68	0.62	0.63	0.92
P9	0.00	0.88	0.39	0.82	0.00
P10	0.90	0.96	1.00	0.75	0.56
P11	0.33	0.50	0.84	0.21	0.00
P12	0.78	1.00	1.00	0.60	0.00
P13	0.42	0.00	0.13	0.41	0.00
P14	0.00	0.97	0.46	0.00	1.00
P15	0.16	0.35	0.45	0.36	0.89
P16	0.92	0.97	0.81	0.05	0.14
P17	0.00	0.00	0.88	0.18	0.28
P18	0.05	1.00	0.63	0.00	0.77
P19	0.62	0.05	0.80	0.27	0.30
P20	1.00	0.69	0.01	0.50	0.48
P21	1.00	0.17	0.39	0.17	0.00
P22	0.35	1.00	0.00	0.70	0.51
P23	1.00	0.68	0.83	0.45	0.00
P24	0.06	0.45	0.82	0.59	0.00
P25	0.15	0.46	0.67	0.49	0.04
P26	0.74	1.00	0.91	0.68	0.00
P27	0.94	0.55	1.00	1.00	0.94
P28	1.00	0.00	1.00	0.34	0.00
P29	0.97	0.37	0.08	0.00	0.27
P30	0.10	0.69	0.00	1.00	0.53
P31	0.95	0.08	0.50	0.46	0.07

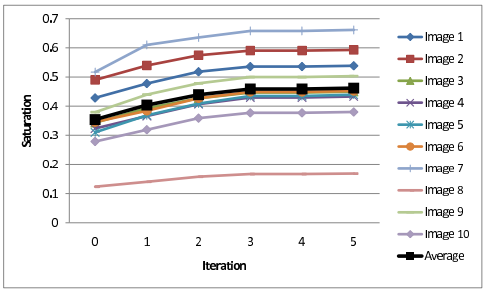

Figure 3: Multiple iterations of saturation enhancement.

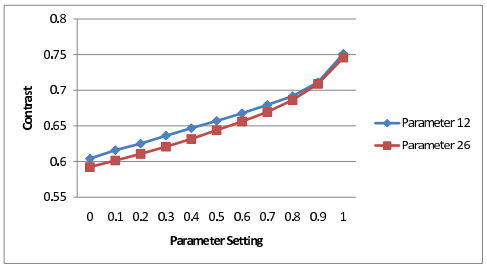

Figure 4: Contrast parameters with direct proportionality.

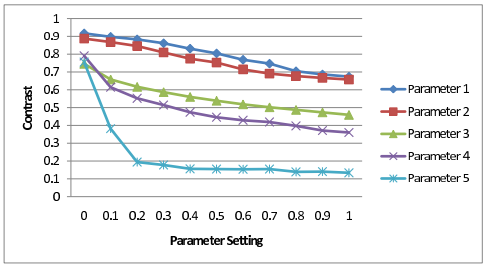

Figure 5: Contrast parameters with inverse proportionality.

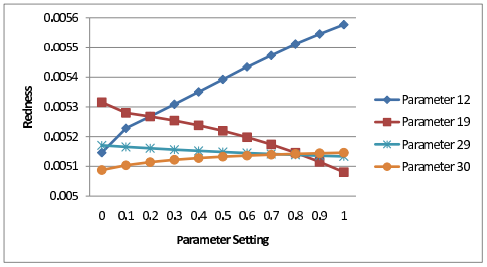

Figure 6: Redness parameters.

portional to contrast, whereas the second one depicts parameters that are inversely proportional to contrast. Notice how different parameter/contrast curves exhibit different degrees of linearity and steepness.

Figure 6 presents several parameters whose modulation affects the level of redness in processed images. The different curves reveal different types of relationship (i.e. direct or inverse proportionality), degrees of linearity and steepness.

DISCUSSION

The results indicate that the OPL-inspired LRNN is stable (see Figures 2 and 3) and does indeed exhibit functional versatility (see Table 2). The model is capable of modulating noise, brightness, contrast, saturation and colour. Table 2 demonstrates that optimized solutions can generalize to new images. According to these results, the strongest functions are ↓ noise, ↑↓ contrast and ↑↓ saturation, whereas the weakest ones are ↑↓ brightness and colour correction. It is possible that a slightly more complex model (e.g. incorporating further biological nonlinearities) might allow for more effective brightness normalization and color correction.

Due to space constraints, an in-depth analysis of the parameter variations in Table 3 is not possible. However some observations can be made. Notice how parameters P3 and P4 tend to be larger in the ↓noise solution relative to the other solutions. This is due to the averaging (and thus denoising) effect of the corresponding GJs. P3 is also relatively large in ↓saturation because this parameter directly contributes to the pulling of chromaticities towards a central grayer value. In the ↓saturation solution, notice how the HC layer seems to be effectively switched off (e.g. the HC3-PR weight (P26) is zero and the HC1 output radius (P7) is zero). Further tests of the degree of impact of different HC types on the PR layer confirmed that in the ↓saturation solution only HC2 had an impact. In the ↓noise solution the desaturating effect of P3 is counteracted by a saturating effect implemented by the HC layer (all HC types have an impact on the PR layer). This saturating effect mirrors what is found in the ↑saturation solution. First of all, notice how in the ↑saturation solution P3 is zero (in contrast to ↓saturation). Secondly, notice how HC2 (i.e. the second HC type, counting from the top of the table) is effectively unused: the input weight is zero and the output radius is zero. The two remaining HC types are differentiated in terms of receptive field size (one large and one small) and chromatic properties (the order of RGB proportions in one HC type is the reverse of the order in the other). Thirdly, notice how inter-positional HC GJs are *zero* for the same HC type but *one* for different types. The ↑contrast solution is quite similar to the ↑saturation solution. HC impact tests revealed that all HC types had an effect on the PR layer, although HC2 did have a significantly weaker impact than the other HC types. HC1 and HC3 exhibit different receptive field sizes and inverse orders of RGB proportions. The HC input/output weights are approximately $0.5/1.0$ for both HC types. The HC GJ configuration in the ↑contrast solution is relatively distinct from the ↑saturation solution, however since both solutions do their processing in a single iteration (see P31), thus making the effects of HC GJs not apparent at the PR layer until iteration 2, nothing can be concluded from their different settings. The simple ↓contrast solution appears to be mostly a consequence of parameters 1 to 4 being zero.

The results also show that the visual functions can be modulated either by running variable numbers of iterations (e.g. Figure 2) or by modulating specific parameters. Figure 4 shows that by increasing/decreasing the weight of connections from HC to PR cells, we can increase/decrease contrast. Ideally we would like to have a minimal subset of parameters, which is amenable to logical manipulation, such that any of the functions (e.g. color correction) can be activated to any degree (e.g. large gradations) and in any way (e.g. remove blue illuminant). The current paper demonstrates initial steps in this direction.

The fact that saturation related solutions seem to re-

quire fewer HC types than contrast related solutions might contribute to answering the question of why the human retina seems to exhibit 3 HC types contrary to many other mammalian retina. The experiments also revealed that even in cases where HCs might have no direct impact on the PR layer they may still be crucial in an indirect manner, e.g.: if a HC does not receive input from the PR layer it may do so (indirectly) from neighboring HCs and then output this information to the PR layer or if a HC does not output information to the PR layer, it may receive information from it and then feed it back (indirectly) via neighboring HCs.

CONCLUSION

Some of the strengths of the OPL-inspired multi-resolution LRNN include: generality, parallelizability, simplicity, versatility, adaptability, extensibility and biological relevance. Generality is verified by the fact that the LRNN performs as expected on new images. Parallelizability is an automatic consequence of the LRNN being a neural solution. Because the LRNN consists of a mere two layers we can say that the solution is simple. Versatility results from the fact that the LRNN can be optimized for several different functions involving noise, brightness, contrast, saturation, color and possibly other properties. Adaptability ensues from the fact that the LRNN can be effectively modulated in different ways. The fact that the LRNN can be easily modified to incorporate new properties (e.g. salience dependence) suggests that it is extensible.

As the results demonstrate, currently the weakest functions seem to involve color correction and brightness control. These weaknesses might be linked to another limitation, which refers to the chosen level of abstraction. By incorporating other OPL details and thus expanding the currently restricted parameter space, the above limitations might be solved and new functions might be realizable (e.g. saliency mapping).

Future work thus includes: expansion of the model, improvement of brightness and color correction, exploration of new low-level visual functions, deeper analyses of parameter settings and their effects on different functions, inclusion of more realistic temporal properties and development of a theory of the network's dynamics, analysis of patterns of indirect HC effects, exploration of algorithmic extensions, generation of biological hypotheses with broader implications and refinement of the function control space. The last point refers to the ability to efficiently modulate parameters such that different functions and function combinations can be activated in different ways and degrees using a minimal parameter subset. The ultimate objective is to automate the modulation of this parameter subset and relate this to plausible OPL functions such as contrast gain control.

REFERENCES

Ebner, M. (2006). Evolving color constancy. *Pattern Recognition Letters*, 27(11):1220–1229.

Egmont-Petersen, M., De Ridder, D., and Handels, H. (2002). Image processing with neural networksa review. *Pattern Recognition*, 35(10):2279–2301.

Field, G. and Chichilnisky, E. (2007). Information processing in the primate retina: circuitry and coding.

Goldberg, D. (1989). *Genetic Algorithms in Search and Optimization*. Addison-wesley.

Haykin, S. (2008). *Neural networks: a comprehensive foundation*. Prentice Hall.

Kolb, H., Fernandez, E., Schouten, J., Ahnelt, P., Linberg, K., and Fisher, S. (1994). Are there three types of horizontal cell in the human retina? *Journal of Comparative Neurology*, 343(3):370–386.

Masland, R. (2001). The fundamental plan of the retina. *nature neuroscience*, 4:877–886.

Schutter, E. (2009). *Computational Modeling Methods for Neuroscientists*. MIT Press.

Storn, R. and Price, K. (1997). Differential evolution–a simple and efficient heuristic for global optimization over continuous spaces. *Journal of global optimization*, 11(4):341–359.

Wohrer, A., Kornprobst, P., and Vieville, T. (2006). From light to spikes: A large-scale retina simulator. *Proceedings of the IJCNN 2006*, pages 8995–9003.

Zaghloul, K. and Boahen, K. (2006). A silicon retina. *Journal of Neural Engineering*, 3:257–267.

AUTHOR BIOGRAPHIES

TOMÁS H. MAUL was born in Madeira, Portugal and did a BSc. in Biological Psychology at the University of St. Andrews, an MSc. in Computer Science at Imperial College and a PhD. in Computational Neuroscience at the University of Malaya. He worked for two years at MIMOS Bhd. as a Senior Researcher in the fields of Pattern Recognition and Computer Vision. He is currently an Assistant Professor at the University of Nottingham Malaysia Campus, where he conducts research in the areas of Neural Computation, Optimization and Computer Vision. His e-mail address is `Tomas.Maul@nottingham.edu.my` and his Web-page is `http://baggins.nottingham.edu.my/~kcztm/`.

ANDRZEJ BARGIELA is Professor and Director of Computer Science at the University of Nottingham, Malaysia Campus. He is a member of the Automated Scheduling and Planning research group in the School of Computer Science at the University of Nottingham. Since 1978 he has pursued research focused on processing of uncertainty in the context of modelling and simulation of various physical and engineering systems.

His current research falls under the general heading of Computational Intelligence and involves mathematical modelling, information abstraction, parallel computing, artificial intelligence, fuzzy sets and neurocomputing.

LEE JUNG REN is currently pursuing his PhD in Computer Science at The University of Nottingham, Malaysia Campus. He did a Bachelors of Computer Science in the same university in 2007 where he developed a Medical Diagnosis Aiding application with Semantic Web for his Final Year Dissertation. His current research is focused on a neuroalgorithmic approach to retinal modeling.